Potential Safe Plasma Termination Using Laser Ablation of High-Z Impurity in Tokamak

Y.Z.Zheng, Q.W.Yang, A.K.Wang, X.Y.Feng, Y.Huang, H.Wang

Southwestern Institute of Physics, P.O.Box 432, Chengdu, Sichuan, 610041, China
yz.zheng@swip.ac.cn

Abstract. Major plasma disruptions are considered to be a serious problem for development of tokamak fusion reactors. The preliminary experiment results in HL-1M and HL-2A presented here describe the methods of amelioration of plasma current quench in major disruptions using laser ablation of high-Z impurities, which support the design of next generation large tokomaks like ITER. Using injection of impurity with higher electric charge allows us to increase the radiation cooling. Resistive, highly radiating plasma formed prior to the thermal quench, can dissipate both the thermal and magnetic energy. It can be possibly a simple and potential approach to decrease significantly the plasma thermal energy and magnetic energy before a disruption thereby a safe plasma termination is obtained.

1. Instruction

In contemporary large tokamaks, the disruptive termination of a discharge can reduce the lifetime of the first wall materials because they are irradiated by the intense heat flux at the energy quench and bombarded by energetic runaway electrons during the current quench, and generate high electromagnetic forces acting on vacuum vessel components due to the intense eddy current and halo current at the current quench. Thus, it is necessary to avoid or mitigate the energy quench and the current quench, and to control an anticipated disruption or emergency shutdown in the large tokamak machines.

The thermal energy and the magnetic field energy associated with the plasma current must be dissipated safely when a discharge is terminated in disruption. [1] The magnetic energy can be dissipated by impurity radiation if plasma position control is maintained. [2] The thermal energy is usually conducted to the plasma contact points in about 0.2-0.5 ms time period for a thermal quench prior to the dissipation of magnetic energy. Therefore, resistive highly-radiating plasma formed prior to the thermal quench could dissipate both the thermal and magnetic energies and minimize the risk of local deposition. Using the injection of impurities with higher electric charges can produce resistive highly radiating plasma and increase the radiation cooling of plasma to make a safe termination of the disruption. There appears an approach to reducing significantly the plasma thermal energy before a disruption. A high-*Z* impurity (KCl) pellet injection has been used in such an application on T-10 [3] and noble gas jet injection has been used for disruption mitigation on DIII-D. In this paper it is reported that a preliminary experiments are performed in HL-1M，HL-2A using the injection of Al or Ti by laser ablation to investigate this approach. By analyzing features of the MHD perturbations, a new criterion is introduced to predict the major disruptions. In addition, a primary off-line neural network is developed to cross-check disruption prediction.

2. Experimental Results

The main idea of the experiments is to obtain resistive highly radiating plasma formed

prior to the thermal quench and increase the efficiency of plasma cooling due to high-*Z* impurity radiation. The radiation source is created by laser ablation of Al or Ti. Laser beam with energy output of 2-5 *J* and pulse duration of 20 ns focused on the metal films with 10 μm in thickness and produce a burst of metal gas, which moves towards the plasma center. Figure1 shows the laser blow-off system. The laser spot with a diameter of 3-5 mm contains a few 10^{19} atoms of metalline element. When those metallic atoms move towards the plasma confinement region, they experience a series of processes: ionization, collision and diffusion.

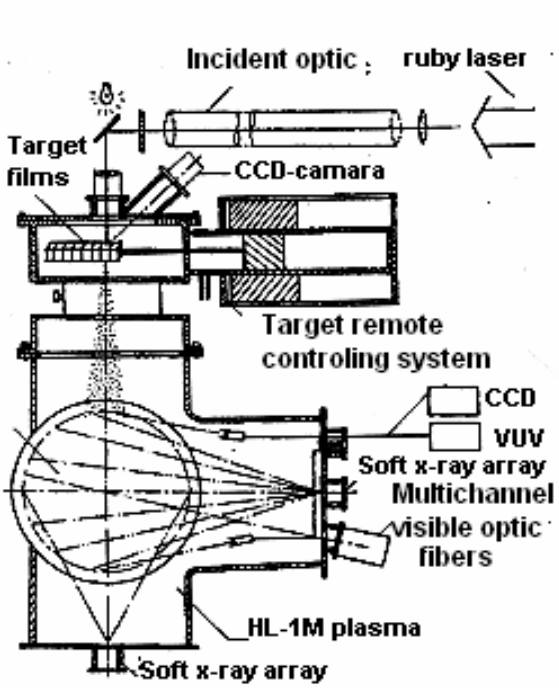

Fig.1. The laser blow-of system

If the ions at various ionization levels of injected impurities wholly distribute in core confinement region, the ion density well is occupy 0.5-2% of the electron density in plasma center region (r/a<1/5),[4] which can be demonstrated by absolute measurements from the VUV (Vacuum Ultra Violet) spectrometer with the impurity transport code SITCODE simulation. [5] In fact，only a fraction of such ions can reach the center. The target chamber is attached to the top of the vessel and the injection point is approximately 0.9 m from the plasma boundary. The injected neutral particles have a measured energy of a few *eV* and reach the plasma boundary in less than 1 ms. The neutral atoms are ionized on the plasma edge and spread out rapidly along the field lines. At the same time, because of collisions or turbulence, the ions move slowly and radially inwards typically at speeds of 1-10 m/s that are measured with the CCD-camera. The penetration of the impurities into plasma is observed using two soft x-ray imaging cameras and a CCD-camera. The penetration radius is about 20 cm measured by the CCD-camera, or evaluated from the ionization levels of injected impurities (Al^{10+}, Al^{11+} and Al^{12+}) measured with the VUV spectrometer. The impurity particles normally travel inward half of the minor radius and creates a maximum impurity deposition there. The plasma parameters before the injection are as follows: plasma current Ip is 150 kA, toroidal field B_t is ~ 2T, central electron temperature $T_e(0)$ ~ (0.6-1.2) keV, line-averaged electron density $\bar{n}_e$ ~ 2-3×10^{19} m^{-3}.

The plasma behaviour varies with the quantity of injected impurity and the plasma density. The injection of a small amount (<0.01%) of the electron density causes a slight perturbation of $\triangle n_e/n_e$ ~ 0.05, $-\triangle Te/Te$ ~ 0.2. Such plasma parameters as $T(r,t)$, loop voltage $V_l(t)$ are relaxed in 20 - 30 ms to new steady-state levels which are close to those prior to the injection. No changes in m = 2 MHD (magnetohydrodynamic model) activity or in 'Hard x-ray' signal (HXR emission with energy more than 3 *MeV*) are observed.

The plasma behaviours after the injection of a larger amount of Al can be divides into three phases, as shown by vertical lines in Fig.2.

In the phase Ⅰ - impurity entry and loss of the thermal energy, the Al plasma forms. It

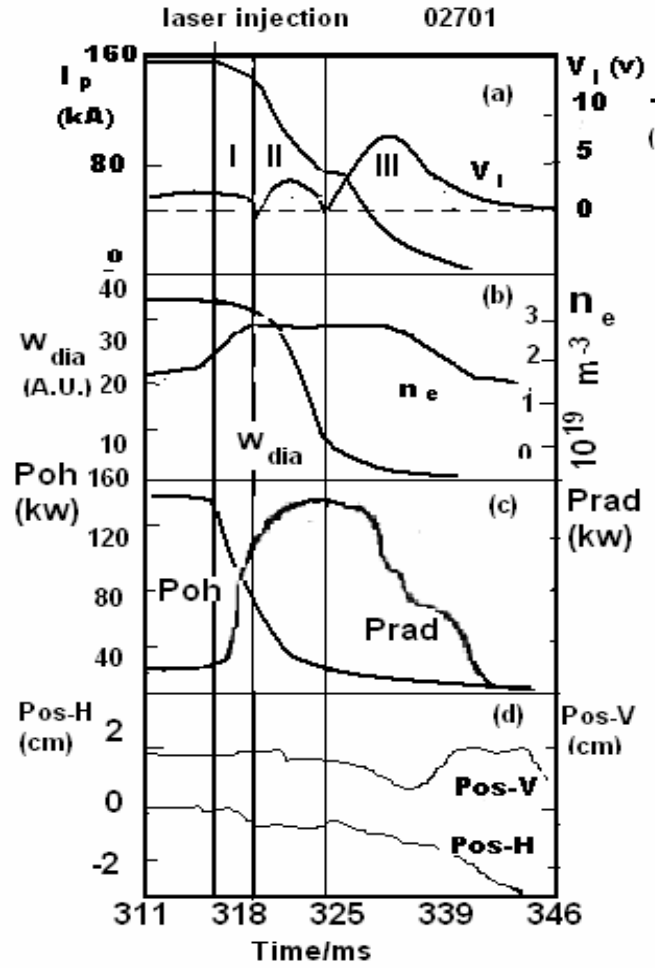

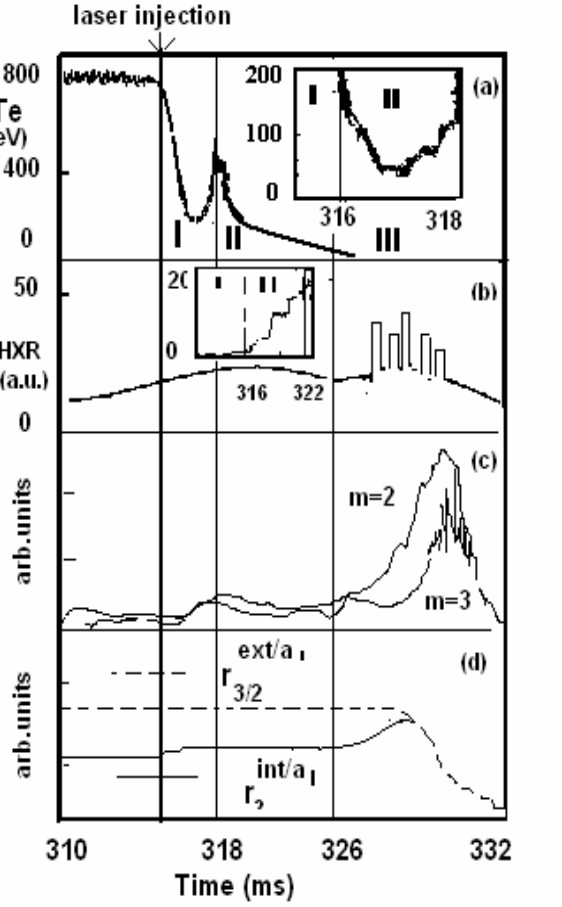

takes at least 2-3 ms to ionize the injected Al and undergo the mass toroidal deposition and then achieve the toroidal-poloidal symmetrization of the electron density, which can be estimated from the rise and saturation times of the interferometer signals $\bar{n}_e$(see Fig.2b). In this phase, current starts to decay and then the plasma horizontal position moves about 1.2 cm at a roughly constant rate, which is indicative of loss of thermal energy. The current decreases by ~20 *k*A in 2 ms and the negative loop voltage spike with 0.3 ms duration is observed. The perturbations in poloidal and radial fields appear and grow but only up to moderate amplitude. In this stage, the total power radiated significantly increases (see Fig.2c, signals are measured by the barometer) and the loss of thermal energy occurs, then significant temperature perturbation in the ambient plasma reaches (-$\triangle Te/Te$) ~ 0.5-0.9 ($\Delta\bar{n}_e/\bar{n}_e$ ~ 0.15-0.5) due to deposition of impurities. The electron temperature drop is measured by using the ECE (Electron Cyclotron Emission receiver) as shown Fig.3a and the soft X-ray PHA (Pulse Height Analysis) analyzer. The magnitude of the temperature drop is roughly proportional to the number of electrons deposited. The loss is also indicated by the plasma β in the equilibrium analysis reducing to vicinity of zero and the resulting horizontal shift of the plasma. The loss of total plasma pressure measured by diamagnetic loops is observed as

shown in Fig.2b. It is indicated in this cold, high density, post Al-injection discharges that both electron and ion thermal energies are lost on the same time scale. The phase Ⅰ ends with a minor disruption. The duration of the phase varies within 2-25 ms time range and increases with decrease of laser power and thickness of metal films or the plasma density. The phase Ⅱ -Current beginning to decay at a decay rate of ~30 kA/ms. It corresponds to a Spitze resistivity temperature of ~10eV. The loop voltage becomes positive and significantly increases. We have observed a significant reduction in the plasma energy content △W / W, the reduction is measured to be about 80% of its maximum value in shot #02701. In this phase, the growth of the perturbed magnetic field is essentially completed. As a result of plasma cooling the vertical position control is switched off, but the vertical position is essentially unchanged. The horizontal position shifts inward (see Fig.2d). It is seen from Fig.3c that before disruption, the amplitudes of mode m=2(q=2) and later mode m=3(q=3/2) grows up and are measured by using MHD Fourier techniques. The second sharp drop of the electron temperature T_e and a steady increase in hard x-ray rate are observed. The increase is presumed to reflect a gradual buildup of energetic electrons during the initial current decay. With the further increasing of the loop voltage, the electron temperature reaches its minimal value. We simulate the evolution of the current density profile j (r,t) after the impurity injection by using the diffusion equation for a poloidal magnetic field. The neoclassical plasma conductivity is calculated using experimental profiles $T_e(r,t)$ and $n_e(r,t)$. The simulated j(r,t) profiles then serve as the input data for the code to calculate stability and parameters of magnetic islands. [6] The simulation results have shown that all modes with the poloidal number m>4 are stable at all the times while the m=2, 3, 4 modes are still developing. The time behaviour of the external boundary position of the m=3 (q=3/2) $r_{3/2}^{ext/a}(t)$ island and the internal boundary position of the m=2 (q=2) $r_2^{int/a}(t)$ island are shown in Fig.3c. It is seen that the disruption occurs at the moment when the q=2 and the q=3/2 islands are intercepted. This implies an appreciable influence of the j(r,t) evolution on the disruption development.

In the phase Ⅲ, current decay ends. A small non-thermal current appears and the total current increases by 10 kA that is above an extrapolated value from the resistive decay. An extended period of negative loop voltage appears. The vertical position then returns to vicinity of the vessel center, the current decay rate returns to 20 kA/ms and the discharge terminates on the inner wall. The electron energy content is not restored after the disruption.

The soft x-ray emission during the injection is carried on in two stages, illustrated in Fig.4. After ablation of the injected impurity, the radiation profile builds up at minor radius immediately, with no growth in radiation from the center. In the central region no sawtooth crash occurs. [7] Then it takes 2-3 ms for the radiation profile to become peaked on axis.

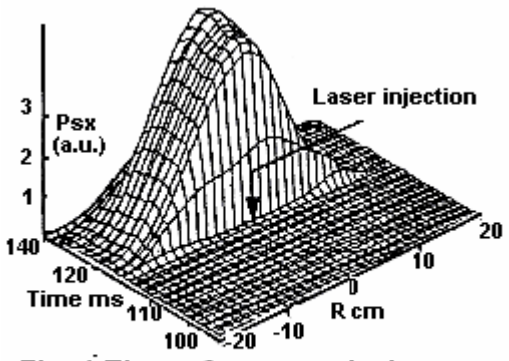

Fig. 4 The soft x-ray emissions during the injection in two stages

3. Discussion

The experiment demonstrates a possibility of fast (3ms) plasma cooling and losing about 80% of plasma energy before disruption occurs. The plasma resistance before the current decay is calculated by equating the ohmic dissipation to the known input power. If the plasma resistivity is Spitzer resistivity of this kind, taking *Zeff* = 4, the electron temperature in HL-1M in 2 ms before the current decay is inferred to be ~10 eV. The lowest *Te* is < 40 eV, which could be achieved by anomalous conductivity before the disruption. The drop in *Te* at the moment of disruption is due to not only the enhancement of transport across the minor radius but also the radiation cooling. Before the disruption an influx of impurity atoms would cool the plasma while they are ionized, causing the temperature to drop. Figure2c shows a comparison between ohmic heating power (P_{oh}) and radiation power (P_{rad}). Both thermal energy and magnetic energy appear to be dissipated largely by radiation. The electron temperature drop is simulated by the simple code. [7] The plasma equilibrium calculations are obtained at the end of phase Ⅱ using the ZYZ equilibrium reconstruction code [4] with a high time resolution (~0.2 ms). The plasma equilibrium is well maintained through the loss of thermal energy and the initial loss of magnetic energy in the initial phase of current decay. The horizontal position of plasma shifts inward during the loss of thermal energy and plasma current, and the vertical position are essentially unchanged.

The current plateau during the current decay shown in Fig.2 has a standard feature of fast disruption with low density ($\bar{n}_e \sim < 0.8\times10^{19}$ m^{-3}) in HL-1M. The plateau results from a current carried by runaway electrons, and the number of runaway electrons generated can be used as an indication of T_e. Calculations of the rate of generation of runaway electrons show the Dreicer field, E_D, induced. If T_e is dropped during the impurity injection, a larger electric field is induced, and then growth of a small thermal current is observed. Simulations using the Parail-Pogutse approach [8] and the 'avalanching effect' [9] have shown that when the large drop of *Te* has occurred, the runway generation should take place just after the minor disruption. The current carried by runaway electrons is low, so increases only by 10kA that is above an extrapolated value from of resistive decay. Since runaway electron current touching the components of the first wall can cause their damage. Therefore, it must be careful to use the mitigation technique that suppresses generation of runaway electrons during the impurity injection. Some experimental techniques such as intensive massive neon or helium puff have been applied. The experiment with an extremely applied magnetic error field and auxiliary plasma heating will carry out in HL-2A. Unlike the external magnetic field perturbations, the massive neon or helium gas puffs into disruptive plasma that can efficiently prevent the runaway electrons from being generated in HL-1M. The analysis of experimental data has shown that these disruptions are characterized by a very fast increase in the plasma density, thus reduction in generation rate of runaway electrons also can extend the current quench stage, with the induced plasma current decrease (Fig.5.). These methods need to further study.

The radial vessel displacements at the top and bottom of the vessel measured at 4th toroidal locations with an accurate vibration measuring instrument (precision: 0.1 mm) show that the magnitude of the displacement produced by laser ablation of high-z impurities that can cause current termination is small and almost symmetric, indicating that a little impact of the laser ablation of impurities take place. Though, vessel has ripple section, the received power is symmetries, as a whole, the influence of displacement is less. The vacuum vessel

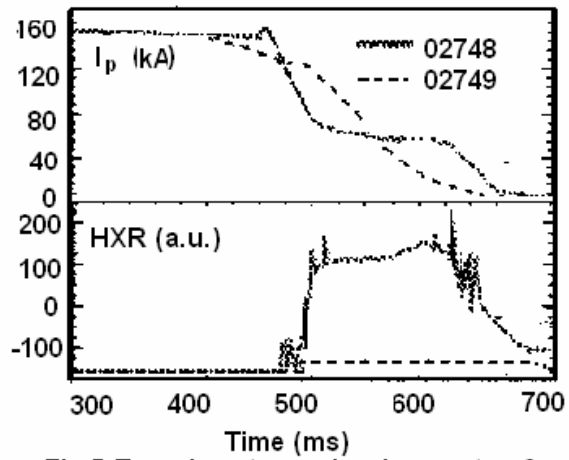

Fig.5 Experiments on developments of runaway suppression techniques using programmed inert gases puff. Temporal evolutions of plasma currets, hard X-ray (HXR) for disruptions #02749 are compared with these for neon puff and for #2748-without gas puff

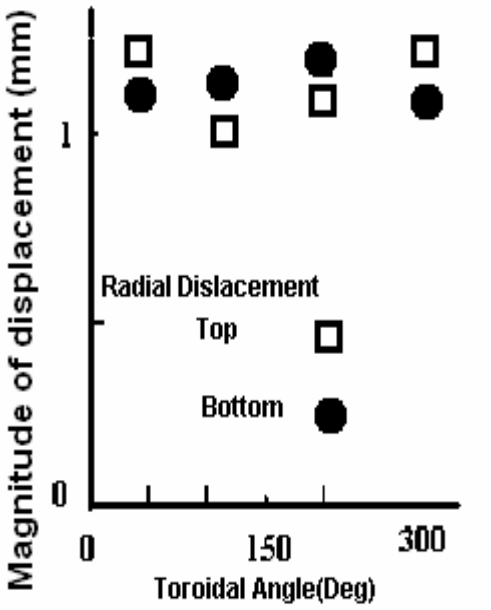

Fig.6 Radial vessel displacement

displacements indicate the severity of the force that is toroidally symmetric during a disruption as shown in Fig.6.

4. Disruption Forecasting

Disruption prediction is carried out in the HL-2A tokamak, using an artificial neural network and the parameter of MHD perturbation: $\delta B_\theta \cdot \tau_p$.

The best network configuration is composed of 13 inputs, 1 output, and three hidden layers with 15, 15 and 10 hidden neurons, respectively. 13 diagnostic signals are taken as the inputs. The trained network has successfully forecasted the disruptive events.

According to the statistic analysis of MHD perturbation and disruption, a new parameter, $\delta B_\theta \cdot \tau_p$, is introduced to predict disruption. Where, δB_θ and τ_p are respectively the amplitude and period of MHD perturbation field detected by Mirnov coil. It is successfully predicted that there are more than 95% disruptions. If assisted by some disruption warner by means of MHD Fourier analyzer, a kind of method to avoid and soften the energy quench and the current quench and control an anticipated disruption or emergency shutdown can be developed in the HL-2A tokamak.

5. Conclusions

1) The injection of high-*Z* impurity into the ohmicly heated HL-1M plasma shows a possibility of fast (~3ms) plasma cooling and losing about 80% of the energy before the disruption occurs.

2) Large amounts of high-*Z* impurities are chosen, with the purpose of enhancing the Z_{eff} in the plasma center at high *Te*, and producing a large electron density perturbation, both of which can provide a strong radiation source and reduce the background electron temperature immediately below 0.1 keV by dilution.

3) The experimental results indicate that a resistive, highly radiating plasma formed prior to the thermal quench, could dissipate both the thermal and the magnetic energies with little

MHD activity present and minimize the risk of local deposition.

4) The growth of a non-thermal current due to runaway electrons is observed. The runaway electrons generation occur during the minor disruption due to the larger Dreicer parameter $E/E_D \sim 0.0025$ before the impurity injection, and experiments using additional methods to suppress this current should be tested. The generation of runaway electrons can be reduced easily by using an intensive massive neon or helium puff and externally applied magnetic field perturbation or increasing the background electron density.

References

[1] Wesson J A Gill R D and Hugon M, Nucl. Fusion Vol. 29, (1989)641
[2] Yamazaki K and Schmidi G L, Nucl. Fusion **24**, 4,(1984)45
[3] Kuteev B V Sergeev V Yu and Sudo S, Nucl. Fusion **35**, (1995) 397
[4] ZHENG Y Cao Z and Li W, Nuclear Fusion and Plasma Physics, **22** (1), (2002)17(in Chinese)
[5] Luo C X Li K F and Wang Q M, Research using small tokomaks, Presented at IAEA Technical Committee Meeting, (1991)82
[6] Chudnovskij V Yu, IAEA-R-887/6(1984)
[7] Dong G F, Shi B R, Li W and Luo J L, Chinese Physics **13**(3) (2004) 379
[8] Parail V V and Pogutse O P, Reviews of plasma physics, **11** (1986) 1
[9] Jayakumar R, Fleschmann H H and Zweben S J, Phys. Lets. A **172(**1993) 447

Figure Captions

Fig.1 Shows the laser blow-off system.
Fig.2 The plasma behaviors after the injection of Al
Fig.3 Te from ECE emission at center (a), hard x-ray signal from Nal scintillator (b) MHD behaviors and q=2 and q=3/2 islands intercepted after the injection (c)
Fig.4 The soft x-ray emissions during the injection in two stages
Fig.5 Experiments on developments of runaway suppression techniques using programmed inert gases puff. Temporal evolutions of plasma currents and hard x-ray signal (HXR) for disruptions $^{\#}$2749 are compared with these for neon puff and for $^{\#}$2748-without gas puff.
Fig.6. Radial vessel displacement